NANO LETTERS

Letter

pubs.acs.org/NanoLett

Dynamic Guiding of Motor-Driven Microtubules on Electrically Heated, Smart Polymer Tracks

Viktor Schroeder,[†,‡] Till Korten,[†,‡] Heiner Linke,[§] Stefan Diez,*[,†,‡] and Ivan Maximov*[,§]

[†]Max Planck Institute of Molecular Cell Biology and Genetics, 01307 Dresden, Germany

[‡]B CUBE—Center for Molecular Bioengineering, Technische Universität Dresden, 01069 Dresden, Germany

[§]Nanometer Structure Consortium (nmC@LU) and Division of Solid State Physics, Lund University, Box 118, 22100 Lund, Sweden

ABSTRACT: Biomolecular motor systems are attractive for future nanotechnological devices because they can replace nanofluidics by directed transport. However, the lack of methods to externally control motor-driven transport along complex paths limits their range of applications. Based on a thermo-responsive polymer, we developed a novel technique to guide microtubules propelled by kinesin-1 motors on a planar surface. Using electrically heated gold microstructures, the polymers were locally collapsed, creating dynamically switchable tracks that successfully guided microtubule movement.

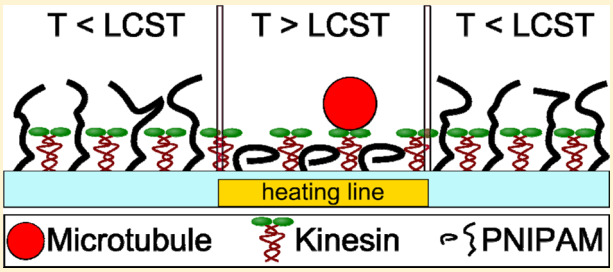

KEYWORDS: *Microtubule, kinesin, poly(N-isopropylacrylamide) (PNIPAM), directional guiding, Y-junction*

Active, chemically powered, biomolecular transport mechanisms are attractive for nanofluidic applications. For example, cytoskeletal filaments, propelled over a surface covered with ATP-hydrolyzing motor proteins, can be used for transporting target analytes to detection areas[1−7] and have been envisioned to power highly parallel biocomputers.[8] For such complex tasks, reliable spatiotemporal control mechanisms are essential. In the past, spatial control over cytoskeletal filaments on a surface coated with motor proteins[9] has been demonstrated by using topographical channels,[10] by patterning motor proteins without topographical guiding walls,[11,12] and by a combination of patterned motors and channels.[13] Temporal control on a global, device level has been demonstrated by controlling the availability of the energy source ATP[14,15] or using the thermo-responsive polymer poly(*N*-isopropylacrylamide) (PNIPAM).[16,17] Electric fields have been used to direct filaments left or right at a topographical junction.[18] However, methods for local, directional control—suitable for integration into complex devices at many guiding points—are still lacking. Here, we present an approach to locally control the motility of gliding microtubules on a planar surface. We use gold lines to locally and temporally heat the thermo-responsive polymer PNIPAM and control the binding and unbinding of microtubules to surface-attached kinesin-1 motors. We demonstrate that we can direct filaments left or right at a Y-branch junction simply by applying a heating voltage to one or the other of the gold lines. The advantage of this dynamic-guiding approach is that it is highly local and, using integrated-circuit technology, is amenable to integration into large-scale, complex devices such as future, programmable molecular-diagnostics and biocomputation devices.

The device concept is shown in Figure 1. The PNIPAM polymer chains are dehydrated and assume a compact conformation in aqueous solution at temperatures above the lower critical solution temperature (LCST; ∼32 °C). When the temperature is lowered below the LCST, the polymer chains are hydrated and extend their contour length several folds. When this polymer is grafted onto a surface, kinesin-1 motor molecules can be adsorbed in between the polymer chains onto the same surface. In the extended state, the PNIPAM chains then screen the motors from solution and prevent the binding of microtubules. When the polymer chains are collapsed, the motors become accessible, and microtubules start to glide.[16] To form narrow, dynamically switchable tracks for microtubules based on the principle of smart polymers, we used the resistive heating of surface-embedded gold electrode structures[19] arranged in a Y-shape. By applying a voltage to either one of the possible branches, the gold lines heat up and collapse the PNIPAM on top of it, switching on microtubule motility along that branch. The microtubule motility can thereby be switched dynamically from one branch to another on a surface without topographical features.

To optimize the design of the silicon chips into which the gold lines are embedded, we first modeled the heat distribution of a cross section of a heated line using the Comsol software (see Figure 2A for a typical heat profile obtained from finite element modeling). We aimed to achieve an optimal compromise between (i) a narrow heat profile with a steep temperature gradient (ideally confining the effect of heating to the widths of the gold electrode itself), (ii) a small voltage to avoid current breakthrough, (iii) a low current density to avoid electromigration, and (iv) an optimized thickness of the

Received: June 2, 2013
Revised: June 5, 2013

dx.doi.org/10.1021/nl402004s | *Nano Lett.* XXXX, XXX, XXX−XXX

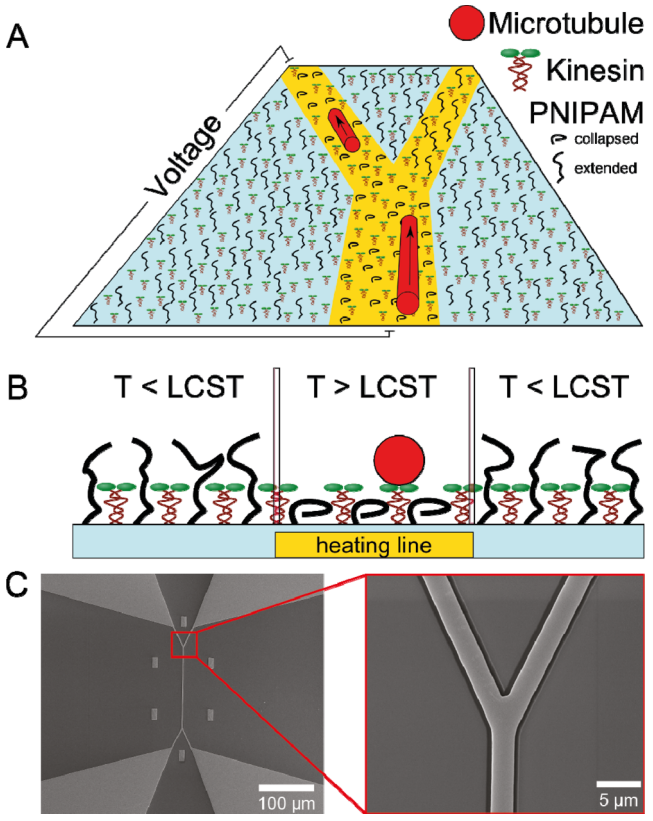

Figure 1. Principle of microtubule guiding along electrically heated, smart polymer tracks. (A) By local heating of a PNIPAM layer, kinesin-1 motors become locally accessible to the microtubules which are then guided along tracks. (B) Cross-sectional view of a surface covered with thermo-responsive PNIPAM and kinesin-1 motors. Joule heating of the gold line causes the PNIPAM to collapse and allows the microtubules to interact with the kinesin-1 motors. (C) Scanning electron microscope image of the gold electrode structure on a silicon substrate.

insulating silicon oxide layer above and below the heated gold line (thicker for better insulating properties but thinner for steeper gradients). The geometry that emerged from our modeling and that was used for all experiments is shown in Figure 2A (see also Materials and Methods).

To experimentally characterize the resistive heating in the vicinity of the gold lines, we used the fact that the enzymatic activity of kinesin-1, and thus the gliding velocity of microtubules, is temperature-dependent (see Figure 2B, method and results similar to refs 20 and 21). Therefore, motility experiments were performed on structured Si chips coated with kinesin-1 and without PNIPAM (see Materials and Methods). The velocity profile of a microtubule gliding across a 2 μm wide heating line (Figure 2C and D) heated electrically (heating power density = 1.5×10^{17} W/m^3) was obtained by microtubule tracking based on the open-source software FIESTA.[22] Using the calibration presented in Figure 2B, the temperature profile in the area of interest was determined (Figure 2E). We found that the area on top of the electrode was heated to 40 °C. The temperature dropped sharply to a plateau temperature of 32 °C at a distance of about 2 μm from the center of the line (ambient temperature: 24 °C). The surface also heated up slightly at larger distances to the line due to heat dissipation. However, the temperature gradient around the heated line was both sufficiently high to cross the LCST of PNIPAM and sufficiently narrow to potentially form tracks suitable for microtubule guiding. In later experiments, the entire chip was cooled using a Peltier element, effectively shifting the temperature profile down in temperature, in order to better match the LCST of PNIPAM.

For the directed guiding of gliding microtubules, motility assays on PNIPAM-coated chips were prepared as described above, except that the chips were heated to 35 °C during the motor incubation step (see also Materials and Methods). During the motility experiments the chip was then cooled by a Peltier temperature stage to 20 °C, so that the temperature on the unheated surface areas was below the LCST of PNIPAM. When we applied a voltage to the 5 μm wide gold electrode (heating power density: 5.6×10^{16} W/m^3), microtubules started to land and glide in the area above the heating line (Figure 3A and B). When the voltage was turned off, the microtubules detached from the surface. To assess the guiding performance of the boundary formed by the transition from collapsed to extended PNIPAM, we investigated the guiding probability as a function of the approach angle. A microtubule was counted as guided when it stayed on the track after a collision with the boundary. When the microtubule detached from the surface after crossing the boundary of the track, it was counted as not guided. Approach angles were binned into intervals, and for each interval the guiding probability was determined by dividing the number of guided microtubules by the total number of microtubules encountering the boundary (Figure 3C). Microtubules approaching under an angle of up to 20° angle had a probability of >80% to be guided. For larger angles the guiding probability decreased and was near 0% at 90°. A total guiding probability of 45% was determined by averaging the values for all angle intervals (bin width = 10°, N = 168 collisions). This value is surprisingly high compared to a previous study where microtubules were gliding toward a protein-repellent polymer barrier (PEG). In that study, a much lower guiding probability of about 12% was reported.[10] One explanation for the better guiding in our case could be the height of the polymers. The PEG layer used by Clemmens et al. was 20 nm thick,[10] which is very close to the height that kinesin carries microtubules over the surface in a gliding assay.[23] In contrast, the extended PNIPAM used here is ~40 nm thick.[16] This increased thickness of the polymer layer adjacent to the guiding tracks (about one microtubule-diameter thicker than in ref 10) potentially contributed to steric guiding. However, given the length and flexibility of the kinesin tails and the softness of the polymer brush, we cannot exclude that some other effects than purely mechanical repulsive forces are at work.

To quantify the guiding efficiency of the track as a whole, we measured the distribution of approach angles for subsequent collisions (Figure 3D). The mean angle at which the microtubules hit the boundary in subsequent collisions (after the first collision) was 24 ± 16° (mean ± standard deviation). The mean guiding probability for consecutive collisions was 75%. Thus, after being guided for the first time, microtubules had a large chance of staying on the track because they approached the boundaries under rather small angles in most subsequent collisions. The probability of a microtubule to reach a specific traveled length decayed exponentially with a characteristic traveled length of (74 ± 11) μm (Figure 3E). This means that 37% ($1/e$) of the microtubules gliding on the track reached this distance.[24] Microtubules traveled at least for a distance as long as their length plus the track width. For this

dx.doi.org/10.1021/nl402004s | Nano Lett. XXXX, XXX, XXX−XXX

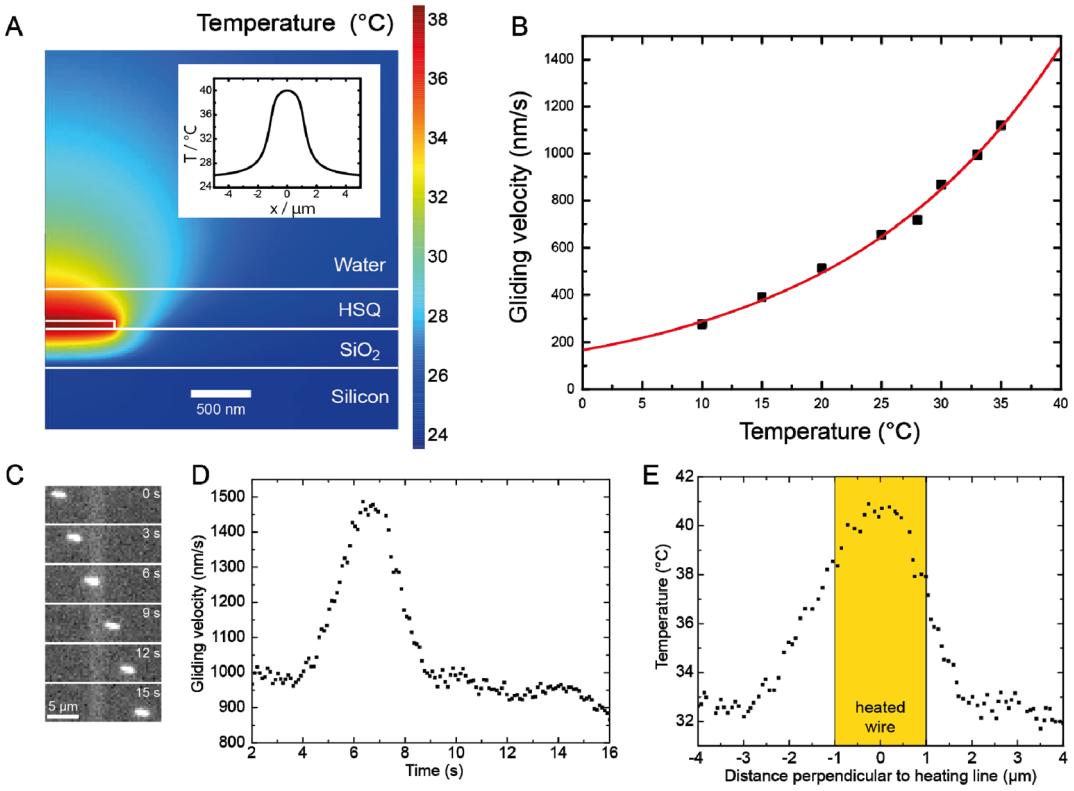

Figure 2. Local heating by the application of electrical currents to gold electrodes. (A) Heat map of a cross section of the heating chip (modeling in COMSOL). Here HSQ (see Materials and Methods) denotes the insulation silicon oxide layer produced by annealing of the HSQ resist. Inset: Temperature profile across the heating line on the surface of the chip. (B) Microtubule gliding velocity in dependence of the surface temperature. The whole chip was heated for this experiment. (C) Image series of a gliding microtubule passing over a heated line. (D) Point-to-point velocity of this microtubule tracked with FIESTA.[22] (E) Heat profile of an electrode measured using the microtubule gliding velocity. The surface is heated up on top of the electrode, but also parts of the surface at a larger distance heat up due to heat dissipation (ambient temperature: 24 °C).

reason the exponential decay begins only after 20 μm of traveled distance.

To demonstrate dynamic switching of microtubule motility, guiding at a Y-shaped junction was investigated. First, we heated only the right arm of the junction. Microtubules that approached the junction were guided into the heated branch by collisions with the extended PNIPAM on the unheated side (Figure 4A). Thus, motility was only observed in the lower branch and the right (the heated) branch of the Y-structure (Figure 4B). When we switched the heating from the right arm to the left arm, motility was only observed in the lower branch and the left (the heated) branch (Figure 4C). Thus, we were able to dynamically reconfigure the guiding tracks on a planar surface. The guiding efficiency at the junction was consistent with that on a straight track when taking into account that microtubules approached the guiding polymer edge at the junction at a steeper angle than on a straight track (average approach angle of 24° plus 25° kink of the channel at the junction). In total, around 57% of the microtubules at the junction were guided into the heated branch, while the other microtubules detached from the surface (Figure 4D). No microtubule was guided into the wrong (unheated) branch, since the extended PNIPAM prevented the attachment of microtubules to kinesin motors reliably. This negligible error rate for the correct guiding direction is especially promising for biocomputation applications, where scalability depends crucially on the error rate.[8]

In summary, we used electrical heating to locally collapse thermo-responsive polymers on top of narrow gold electrodes on silicon chips. Thereby, motility tracks—where microtubules readily interacted with kinesin-1 motors—were formed. Crucially, in addition to the reliable guiding of microtubules along elongated, static tracks we were able to demonstrate the switching of motility between two branches of a Y-junction. We expect that the performance of our demonstrator can be improved by optimizing the geometry (especially the angles) of the switchable junctions. While we focused on exploring the ability of PNIPAM and heat control alone to guide and route filaments, the guiding quality (and the loss rate of filaments) can presumably be drastically improved if PNIPAM guiding is integrated with topographical guiding. In such a system, locally confined polymer pads may also act as gates, where microtubules can pass when the gate is open (i.e., when the polymers are collapsed) or are expelled from the channels when the gate is closed (i.e., when the polymers are expanded). Likewise, such polymer pads may be applicable to topographic Y-junctions, where the conformation of the polymers on a small area will be sufficient to direct the motility into one or the other direction. Being able to freely reconfigure the tracks in an underlying network geometry may boost the applicability of motile bioagents—like gliding microtubules—for programmable biocomputation,[8] such that several distinct mathematical problems will become solvable with a single biocomputation device.

Materials and Methods. Chips with gold heating lines (widths of 2, 5, and 10 μm) were made using a two-inch Si wafer with 327 nm thick SiO_2 as a starting material. After a standard optical lithography in a double-layer resist system

dx.doi.org/10.1021/nl402004s | Nano Lett. XXXX, XXX, XXX−XXX

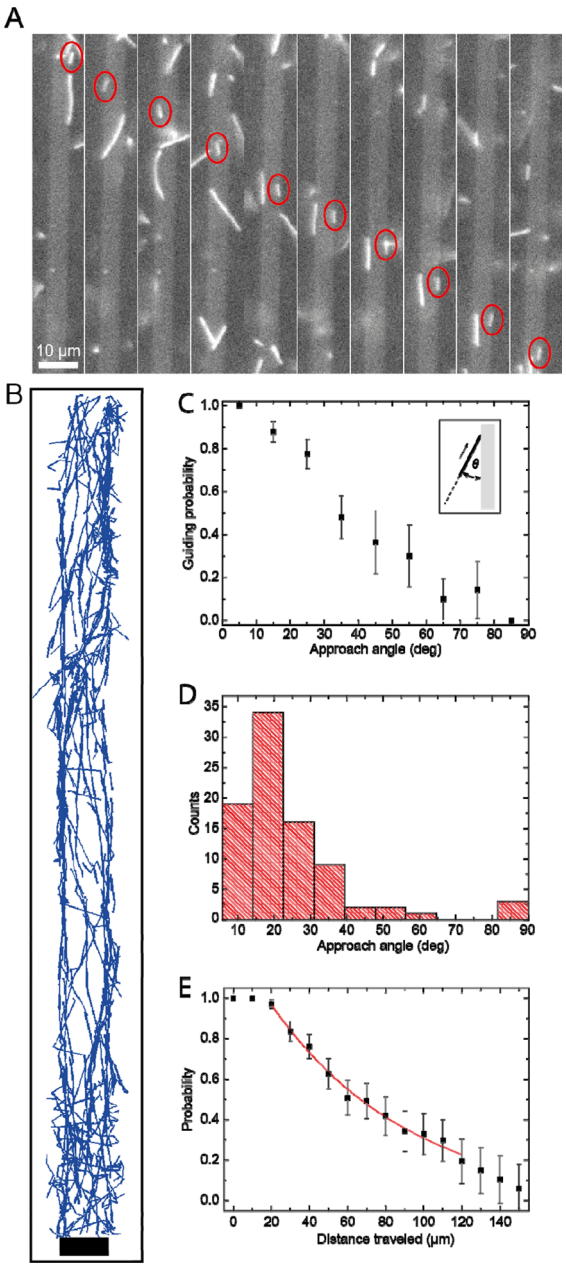

Figure 3. Static microtubule guiding on a kinesin-1 track with thermally collapsed PNIPAM. (A) The marked microtubule is redirected several times during traveling on the PNIPAM track. The time interval between images is 15 s. (B) Paths of microtubules gliding on the PNIPAM track evaluated with FIESTA.[22] Scale bar: 5 μm. (C) Single-collision guiding probability in dependence of the approach angles. Inset: Definition of the approach angle. (D) Histogram of approach angles for collisions subsequent to the first successful guiding-collision. (E) Probability for a microtubule to travel past a given distance in the channel. The exponential part was fitted with a characteristic traveled length of (74 ± 11) μm.

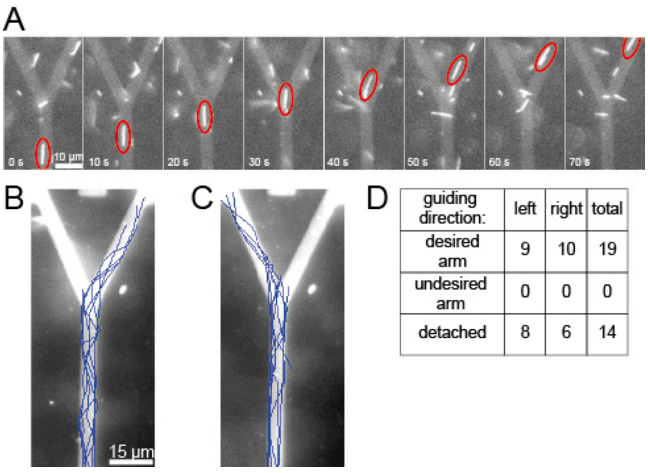

guiding direction:	left	right	total
desired arm	9	10	19
undesired arm	0	0	0
detached	8	6	14

Figure 4. Dynamic microtubule guiding on a kinesin-1 track with thermally collapsed PNIPAM. (A) The marked microtubule approaches the junction and is guided toward the right arm. (B, C) Controlled microtubule guiding into the right or left arm. All microtubules were either guided or detached at the junction. (D) Counts of microtubules being guided into the different arms at the junction. For evaluation, all microtubules passing the line where the lower branch widens (just before the junction) were considered. Microtubules were counted as "guided", when they traveled across the rectangular line between the tip point of the junction and outer wall of either upper branch for a distance at least as long as their own length. Microtubules were counted as "detached", when they left the surface within the described area.

(LOR and S-1813), about 100 nm of silicon oxide layer was etched in a buffered HF-solution to create a recess, followed by a thermal evaporation of 5 nm thick Ti and 100 nm thick Au layers and a lift-off in warm remover S-1165. The wafer was then cleaved into separate chips, which were spin-coated with 240 nm thick hydrogen silsesquioxane (HSQ) resist. The contact areas of the chips were masked by a tape to prevent deposition of HSQ on the contacts pads. Finally, the chips were baked at 350 °C for 1 h to convert the HSQ layer into silicon oxide.

Microtubules were polymerized from rhodamine-labeled porcine brain tubulin[25] in BRB80 (80 mM PIPES, adjusted to pH 6.9 with KOH, 1 mM EGTA, 1 mM $MgCl_2$) with 5 mM $MgCl_2$, 1 mM GTP, 5% DMSO at 37 °C for 30 min. The microtubules were stabilized and diluted 200-fold in BRB80 containing 10 μM Taxol. Flow cells for motility experiments were assembled with the structured chips, two stripes of Parafilm across the surface, and closed with a glass coverslip. The chips were then mounted onto a microscope stage that could be temperature-controlled using a Peltier element.[26] A casein containing solution (BRB80 with 0.5 mg/mL casein) was perfused into the flow cell and allowed to adsorb for 5 min. This solution was exchanged for a kinesin solution (BRB80 with 10 μg/mL Kinesin-1, full length, from *Drosophila melanogaster*, expressed in bacteria;[27] 0.2 mg/mL casein, 1 mM ATP, 10 mM dithiothreitol), which was allowed to adsorb for 5 min. Finally, a microtubule containing solution (motility solution: BRB80 with 10 mM Taxol, microtubules (equivalent of 32 nM tubulin), 1 mM ATP, 40 mM D-glucose, 55 μg/mL glucose oxidase, 11 mg/mL catalase, 10 mM dithiothreitol) was flown in, and imaging was started.

The method for grafting PNIPAM onto a SiO_2 surface was adapted from Ionov et al.[16] Briefly, substrates were cleaned with Piranha solution (70% concentrated H_2SO_4 and 30% H_2O_2 (30% concentrated) *Caution: extremely corrosive and explosive when mixed with organic solvents! Mix slowly pouring cold 30% H_2O_2 into concentrated H_2SO_4*) for 10 min. The clean substrates were then spin-coated (2000 rpm, 500 rpm/s, 30 s) with a 0.01% polyglycidyl methacrylate (PGMA, M_n = 65 000 g/mol) solution in chloroform. The PGMA was annealed at 130 °C for 20 min in a vacuum oven. After annealing the substrates were

dx.doi.org/10.1021/nl402004s | *Nano Lett.* XXXX, XXX, XXX−XXX

placed in hot chloroform (70 °C) in order to remove unbound PGMA. Poly(*N*-isopropylacrylamide) (PNIPAM, M_n = 45 000 g/mol) was dissolved in chloroform (1% solution). The surface of the substrates was then completely covered with a droplet of the PNIPAM solution. After the chloroform evaporated, the substrates were placed in the vacuum oven at 160 °C for 60 min to anneal the PNIPAM. Unbound PNIPAM was removed by washing the substrates in hot chloroform (70 °C).

AUTHOR INFORMATION

Corresponding Author

*E-mail: diez@bcube-dresden.de; ivan.maximov@ftf.lth.se.

Present Address

V.S.: Institute for X-ray Physics and Courant Research Centre "Nano-Spectroscopy and X-ray Imaging", Georg-August-Universität Göttingen, 37073 Göttingen, Germany.

Author Contributions

V.S. and T.K. contributed equally.

Notes

The authors declare no competing financial interest.

ACKNOWLEDGMENTS

The authors would like to acknowledge funding from the European Union Seventh Framework Programme (MONAD, grant 228971), the European Research Council (NanoTrans, ERC starting grant 242933), the German Research Foundation (DFG, Heisenberg Programme and Cluster of Excellence "Center for Advancing Electronics Dresden"), the Knut and Alice Wallenberg Foundation, and nmC@LU. Technical help from M. Graczyk (Lund University), Cordula Reuther (TU Dresden), and Leonid Ionov (IPF Dresden) has been highly appreciated.

REFERENCES

(1) Lin, C.-T.; Kao, M.-T.; Kurabayashi, K.; Meyhofer, E. *Nano Lett.* **2008**, *8*, 1041−1046.
(2) Fischer, T.; Agarwal, A.; Hess, H. *Nat. Nanotechnol.* **2009**, *4*, 162−166.
(3) Ramachandran, S.; Ernst, K.-H.; Bachand, G. D.; Vogel, V.; Hess, H. *Small* **2006**, *2*, 330−334.
(4) Bachand, G. D.; Hess, H.; Ratna, B.; Satir, P.; Vogel, V. *Lab Chip* **2009**, *9*, 1661.
(5) Brunner, C.; Wahnes, C.; Vogel, V. *Lab Chip* **2007**, *7*, 1263.
(6) Schmidt, C.; Vogel, V. *Lab Chip* **2010**, *10*, 2195−2198.
(7) Bachand, G. D.; Rivera, S. B.; Carroll-Portillo, A.; Hess, H.; Bachand, M. *Small* **2006**, *2*, 381−385.
(8) Nicolau, D. V.; Nicolau, J.; Solana, G.; Hanson, K. L.; Filipponi, L.; Wang, L.; Lee, A. P. *Microelectron. Eng.* **2006**, *83*, 1582−1588.
(9) Duke, T.; Holy, T. E.; Leibler, S. *Phys. Rev. Lett.* **1995**, *74*, 330.
(10) Clemmens, J.; Hess, H.; Lipscomb, R.; Hanein, Y.; Böhringer, K. F.; Matzke, C. M.; Bachand, G. D.; Bunker, B. C.; Vogel, V. *Langmuir* **2003**, *19*, 10967−10974.
(11) Reuther, C.; Hajdo, L.; Tucker, R.; Kasprzak, A. A.; Diez, S. *Nano Lett.* **2006**, *6*, 2177−2183.
(12) Bhagawati, M.; Ghosh, S.; Reichel, A.; Froehner, K.; Surrey, T.; Piehler, J. *Angew. Chem., Int. Ed.* **2009**, *48*, 9188−9191.
(13) Van den Heuvel, M. G. L.; Butcher, C. T.; Smeets, R. M. M.; Diez, S.; Dekker, C. *Nano Lett.* **2005**, *5*, 1117−1122.
(14) Hess, H.; Clemmens, J.; Qin, D.; Howard, J.; Vogel, V. *Nano Lett.* **2001**, *1*, 235−239.
(15) Tucker, R.; Katira, P.; Hess, H. *Nano Lett.* **2008**, *8*, 221−226.
(16) Ionov, L.; Stamm, M.; Diez, S. *Nano Lett.* **2006**, *6*, 1982−1987.
(17) Korten, T.; Birnbaum, W.; Kuckling, D.; Diez, S. *Nano Lett.* **2011**, *12*, 348−353.
(18) Van den Heuvel, M. G. L.; De Graaff, M. P.; Dekker, C. *Science* **2006**, *312*, 910−914.
(19) Huber, D. L.; Manginell, R. P.; Samara, M. A.; Kim, B.-I.; Bunker, B. C. *Science* **2003**, *301*, 352−354.
(20) Böhm, K. J.; Stracke, R.; Baum, M.; Zieren, M.; Unger, E. *FEBS Lett.* **2000**, *466*, 59−62.
(21) Kawaguchi, K.; Ishiwata, S. *Biochem. Biophys. Res. Commun.* **2000**, *272*, 895−899.
(22) Ruhnow, F.; Zwicker, D.; Diez, S. *Biophys. J.* **2011**, *100*, 2820−2828.
(23) Kerssemakers, J.; Howard, J.; Hess, H.; Diez, S. *Proc. Natl. Acad. Sci.* **2006**, *103*, 15812−15817.
(24) Clemmens, J.; Hess, H.; Howard, J.; Vogel, V. *Langmuir* **2003**, *19*, 1738−1744.
(25) Gell, C.; Friel, C. T.; Borgonovo, B.; Drechsel, D. N.; Hyman, A. A.; Howard, J. In *Microtubule Dynamics*; Straube, A., Ed.; Humana Press: Totowa, NJ, 2011; Vol. *777*, pp 15−28.
(26) Nitzsche, B.; Bormuth, V.; Bräuer, C.; Howard, J.; Ionov, L.; Kerssemakers, J. W. J.; Korten, T.; Leduc, C.; Ruhnow, F.; Diez, S. *Methods Cell Biol.* **2010**, *95*, 247−271.
(27) Coy, D. L.; Wagenbach, M.; Howard, J. *J. Biol. Chem.* **1999**, *274*, 3667−3671.